

RSC Advances



This is an *Accepted Manuscript*, which has been through the Royal Society of Chemistry peer review process and has been accepted for publication.

Accepted Manuscripts are published online shortly after acceptance, before technical editing, formatting and proof reading. Using this free service, authors can make their results available to the community, in citable form, before we publish the edited article. This *Accepted Manuscript* will be replaced by the edited, formatted and paginated article as soon as this is available.

You can find more information about *Accepted Manuscripts* in the [Information for Authors](#).

Please note that technical editing may introduce minor changes to the text and/or graphics, which may alter content. The journal's standard [Terms & Conditions](#) and the [Ethical guidelines](#) still apply. In no event shall the Royal Society of Chemistry be held responsible for any errors or omissions in this *Accepted Manuscript* or any consequences arising from the use of any information it contains.



RSC Advances

PAPER

Antibacterial and hemostatic composite gauze of N, O-carboxymethyl chitosan/oxidized regenerated cellulose

Feng Cheng,^a Jinmei He,^{*ab} Tingsheng Yan,^a Changyu Liu,^a Xinjing Wei,^a Jiwei Li^a and Yudong Huang^a

The viscose gauze was oxidized with NO_2/CCl_4 to prepare Oxidized Regenerated Cellulose (ORC). Then, ORC was modified by water-soluble chitosan derivative-N, O-Carboxymethyl Chitosan (N, O-CS). This was synthesized via reaction of chitosan with chloroacetic acid as etherification agent in the presence of alkaline. It was prepared by introducing carboxymethyl groups onto the N and O-position of chitosan and the substituting degree (DS) of N, O-CS reached 1.68. Composite gauzes with 2-8w/v % N, O-CS content were prepared in water solution. Composite gauzes could still maintain its original morphological form and have excellent water-solubility. The formation of amide bond between the carboxyl group of ORC and the amino group of N, O-CS was confirmed by FT-IR and Elemental analysis. To study the influence of carboxymethyl groups on chitosan, the thermal stability and crystallinity of N, O-CS were tested by XRD and TG. Based on SEM images N, O-CS tended to be adsorbed on the surface of ORC fiber. Antibacterial performance of N, O-CS/ORC gauzes enhanced with the increase of N, O-CS content. Moreover, N, O-CS/ORC gauzes showed excellent bactericidal activity against both Gram-positive and Gram-negative bacteria. The hemostatic evaluation indicated that the N, O-CS/ORC composite gauzes in rabbit livers had dramatic hemostatic efficacy. The prepared composite gauzes were anticipated to be an optimal material in preventing post-operative adhesion.

www.rsc.org/advances

Introduction

Oxidized regenerated cellulose (ORC) could be obtained by partial oxidation of the primary hydroxyl groups.¹ This is generally used as absorbable hemostatic agents in the vast majority of surgeries. In order to stop bleeding during surgical procedures effectively, ORC containing 16-24 % carboxylic acid content is commercially available in form of powder or sterilized knitted fabric.² Surgical trauma, hemorrhage, inflammation and pathogen contamination may be main causes of adhesions. Based on formation mechanism of adhesion and clinical experience, excellent hemostatic and antibacterial properties are required to prevent postoperative adhesion.³ However, ORC is difficult to ensure that remove all blood from the surgical field⁴ and ORC is mainly used to control low-pressure where the routine methods are not suitable or ineffective in preventing tissue adhesion in the presence of blood or body fluid.^{5, 6} The relatively slow hemostatic rates as well as excessive acidic surface of ORC

limit its wide applications in reducing adhesion.^{7, 8}

Chitosan (CS), a rare positive and alkaline polysaccharide, is well known for its extraordinary biological characteristics-it is nontoxic, nonantigenic, biodegradable, biocompatible, antibacterial, and hemostatic.⁹⁻¹³ However, its poor solubility in physiological solvents severely, limits its further applications in the biomedical field.¹⁴ To overcome the above difficulty, several studies have been successfully prepared water-soluble chitosan derivatives by chemical modification (introduction of carboxymethyl groups on chitosan chains).¹⁵ Among the derivatives of chitosan, N, O-carboxymethyl chitosan (N, O-CS) has shown promising future as anti-adhesion agent, which, can be processed into various forms, including solution, gel, or film. Numerous studies have confirmed that N, O-CS markedly diminishes postoperative adhesion in the pericardial foreign body models. And abdominal cecal abrasion models.¹⁶ In addition, N, O-CS product is efficacious in reducing adhesion formation in cardiac surgery. And N, O-CS products in above forms were biodegradable within 5 days.^{17, 18}

Recent years, few studies have considered C6-ORC gauze as biomedical hemostatic materials, which were coated by chitosan¹⁹ and functionalized multiwalled carbon nanotubes.²⁰ However, no related report involved C6-ORC gauze coated by N, O-CS as postoperative adhesion materials. Compared with the previous research,¹⁷ the N, O-CS/ORC composite gauzes didn't need to be further neutralized with $\text{NaOH}/\text{C}_2\text{H}_5\text{OH}$

^a MIT Key Laboratory of Critical Materials Technology for New Energy Conversion and Storage, School of Chemistry and Chemical Engineering, Harbin Institute of Technology, Harbin 150001, People's Republic of China. E-mail: hejinmei@hit.edu.cn; Fax: +86-0451-8641-4806; Tel: +86-0451-8641-4806

^b State Key Laboratory for Modification of Chemical Fibers and Polymer Materials, Donghua University.

†Electronic Supplementary Information (ESI) available: ¹H-NMR spectra of N, O-CS.

ARTICLE

RSC Advances

solution and could still dissolved in aqueous solution. In this study, the main objective was to prepare a water-soluble gauze with an effective hemostatic and antibacterial material to improve anti-adhesion property. Therefore, N, O-CS/ORC composite gauze was more suitable used for preventing postoperative adhesion in surgery. Briefly, ORC coated N, O-CS composites, C6-ORC gauze was prepared in nitrogen dioxide (NO_2)/carbon tetrachloride (CCl_4) oxidation system. N, O-CS was synthesized from chitosan and chloroacetic acid with appropriate concentration of alkaline. To improve the covalent bond between N, O-CS and ORC the 1-ethyl-3-(3-dimethylamino-propyl)-carbodiimide (EDC), N-hydroxyl-succinimide (NHS) and glycine as cross linking bridges was carried out to fabricate a novel N, O-CS/ORC composite gauze. And N, O-CS/ORC gauzes with different content of N, O-CS were prepared. Then, the structures of N, O-CS and N, O-CS/ORC gauzes were characterized. Finally, the antibacterial and hemostatic properties of composite gauzes were investigated. It is expected that this study could contribute to the design of effective postoperative anti-adhesion barrier material for future applications.

Experimental

Materials

CS (82.5 % deacetylation degree (DD) was obtained from Zhejiang Golden-Shell Biological Co., Ltd., China. Monochloroacetic acid and isopropyl alcohol were purchased from Sinopharm Chemical Reagent Co., Ltd., China. Viscose filament yarn made of regenerated cellulose was obtained from Xinxiang city, Henan province, China. Nitrogen dioxide (AR, 99.99 %, w/w) was purchased from Summit Specialty Gases Co., Ltd., Tianjin City, China. Carbon tetrachloride (AR, 99.5 %) was purchased from Shuang Shuang Chemical Co., Ltd., Yantai City, China. 1-ethyl-3-(3-dimethylaminopropyl)-carbodiimide (EDC) and N-hydroxyl-succinimide (NHS) was purchased from J&K Chemical Co., Ltd. Glycine was supplied by Sinopharm Chemical Reagent Co., Ltd., China. As control Surgicel® absorbable hemostat (commercial oxidized regenerated cellulose) was purchased from Johnson & Johnson Medical Limited. All reagents were used without further purification. Healthy rabbits were supplied by animal experiment center of the second affiliated hospital of Harbin medical university (Harbin, Heilongjiang Province, China). The protocol was approved by the ethics committee of the Harbin Medical University. All animals were handled according to the Chinese National Institutes of Health Guidelines for the Care and Use of Laboratory Animals.

Preparation of ORC

Prior to oxidation, regenerated cellulose filaments were oxidized using the method described in our previous works.^{19, 21} Briefly, NO_2 was dissolved in CCl_4 to prepare 20 wt % NO_2/CCl_4 oxidant, followed by the addition of regenerated cellulose into the flask which contained the mentioned oxidant in a proportion of 1:42.6 ($\text{g}\cdot\text{ml}^{-1}$) (fiber: oxidant). Stirred

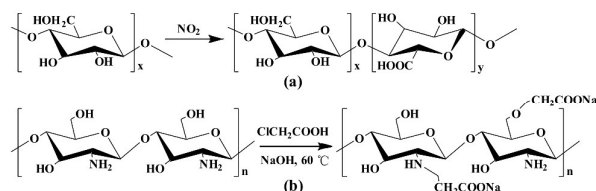


Fig.1 The possible oxidation reaction scheme for the preparation of ORC (a). Scheme illustration for synthesis of N, O-carboxymethyl chitosan (N, O-CS) (b).

constantly, kept the reaction temperature at 19.5 °C and oxidation duration was 40 h (shown in Fig.1a). After the reaction, the product was washed with an aqueous solution containing 50 % (v/v) isopropyl alcohol, and then the product was washed twice or more with 100% isopropyl alcohol. Finally, ORC was frozen-dried at -60°C in vacuum for 24 h.

Synthesis of N, O-carboxymethyl chitosan (N, O-CS)

N, O-CS was synthesized as described in the literature with some modifications.²²⁻²⁴ Briefly, 10 g of chitosan was suspended into 100mL of isopropyl alcohol and the resulting slurry was stirred in a flask at room temperature. 25 mL of 10N aqueous NaOH solution was divided into five equal portions and added to the stirred slurry over a period of 25 min. The alkaline slurry was stirred for additional 30 min. Then monochloroacetic acid (20 g) was added drop wisely in five equal portions at 5 min intervals. Heat was then applied to bring the reaction mixture to a temperature of 60°C and stirring for 3 h. Subsequently, the reaction mixture was filtered and the residue solid product (N, O-CS) was thoroughly rinsed over three times with 80 % v/v ethanol solution and several times with 100 % ethanol. The dry product was obtained by vacuum-drying. The chemical reaction is schematized in Fig. 1b.

DS Measurement

The DS of N, O-CS was measured using potentiometric titration method. N, O-CS (0.2 g) was dissolved in 20mL 0.1mol·L⁻¹ HCl standard solution and titrated by 0.1mol·L⁻¹ NaOH standard solution. Potentiometric titration curve is shown in Fig. 2. The second order micro commercial law was used to get the sudden-change point to calculate the DS of N, O-CS according to the following formulas:

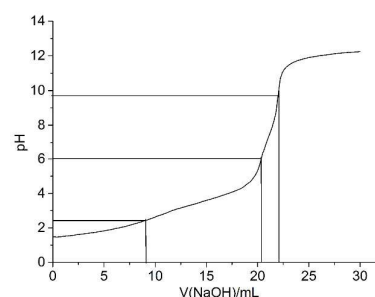


Fig. 2 Potentiometric titration curve of N, O-CS.

$$DS = \frac{0.203A}{1-0.058A} \quad (1)$$

$$A = \frac{(V_2-V_1)C}{m} \quad (2)$$

$$B = \frac{(V_3-V_2)C}{m} \quad (3)$$

$$NH_2\% = \frac{0.203B}{1-0.058B} \times 100\% \quad (4)$$

$$DS_N = DD - NH_2\% \quad (5)$$

$$DS_0 = DS - DS_N \quad (6)$$

Where, V_1 : the potentiometric titration end-point of excessive HCl (mL); V_2 : the potentiometric titration end-point of $-COOH$ (mL); V_3 : the potentiometric titration end-point of $-NH^+$ (mL); C : the molar concentration of NaOH solution (mol/L); m : the weight of N, O-CS (g); DD : the degree of deacetylation of chitosan (82.5 %); DS_N : the DS on NH_2 ; DS_0 : the DS on OH.

Preparation of N, O-CS/ORC Gauze

The optimal group of N, O-CS was used to prepare composite gauzes with ORC, as showed in Fig. 3. N, O-CS solution was prepared through the method of being dissolved in distilled water for 2-8 w/v %. Then, EDC, NHS and glycine was added to N, O-CS solution and stirred using magnetic stirrer for 10min. Finally, the ORC was immersed in N, O-CS solution and stirred at room temperature for 6h. After above treatment, the ORC dipping into the N, O-CS was washed by pressure filtration with 80 % v/v ethanol solution over three times and with 100 % ethanol for several times. Then, modified ORC was frozen-dried at low temperature (223 K) in vacuum for 24 h. The sample of ORC for comparison was also prepared without the addition of N, O-CS.

Characterization of N, O-CS and N, O-CS/ORC Gauze

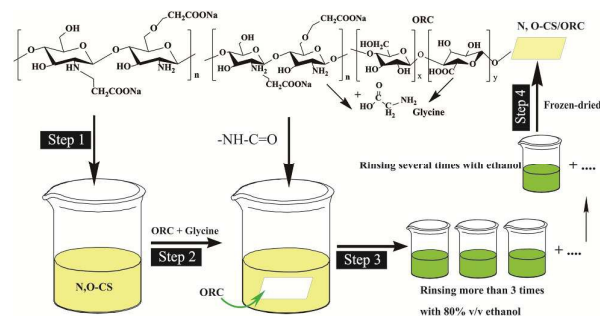
Fourier transformed infrared spectra (FT-IR) proton nuclear magnetic resonance spectroscopy (1H -NMR) were used to confirm the substitutions of carboxymethyl groups on the amino and primary hydroxyl sites of the modified chitosan (N, O-CS). The sample for FT-IR was scanned from 400 to 4000 cm^{-1} . 1H -NMR spectra was performed at room temperature with Varian 400 spectrometer.

Carboxyl group content determination

Carboxyl content was measured according to United States Pharmacopoeia. Firstly, 2 % calcium acetate solution and 0.1 M NaOH standard solution were prepared. Then 0.5 g ORC was cut into short fibers and soaked with 50 mL 2 % calcium acetate solution for 15 h. Using phenolphthalein as an indicator, the above mixture was titrated with 0.1 M NaOH standard solution. And the consumed volume of NaOH standard solution was corrected for blank. Such carboxyl content could be calculated from the following equation¹⁹:

$$-COOH(\%) = \frac{N \times V \times MW_{COOH}}{m} \times 100 \quad (7)$$

Where N is the normality of 0.1 M NaOH solution; V is the consumed volume of NaOH which is corrected for the blank; MW_{COOH} presents the molecular weight of carboxyl group

**Fig. 3** Diagram of the preparation of N, O-CS/ORC composites. and m is the weight of the sample.

Elemental analysis

The carbon (C) and nitrogen (N) contents of composite gauzes and ORC samples were determined by elemental analysis using CHN module of Perkin-Elmer Series II 2400 (USA) CHNS/O Elemental Analyzer. The analysis was repeated for three times. And each sample had the weight range of 1.800–3.200 mg.

X-ray Diffraction

Crystallinity of N, O-CS, chitosan, and composite gauzes was measured by X-ray diffraction method using an XRD-6000X diffractometer with Cu K α X-radiation. The samples were recorded over a diffraction angle (2θ) that ranging from 10° to 60° .

Thermal Analysis

Thermogravimetric analysis (TGA) for N, O-CS, chitosan and composite gauzes were recorded on a SDT Q600 TGA instrument. The samples where weight around 3 mg were heated from 50 to 500 $^\circ C$ at heating rate of 10 $^\circ C/min$ and under the inert atmosphere of nitrogen.

Scanning Electron Microscopy (SEM) Analysis

SEM was used to investigate the surface morphologies of composite gauzes and the connection between N, O-CS and ORC. The samples were sputter-coated with gold for better conductivity during imaging. Then the samples were observed with SEM (Hitachi, S-3400) at the acceleration voltage of 5 kV.

Antibacterial Activity Test

GB/T 20944.3-2008 test method was applied for determining antibacterial activity. Gram positive bacterium, *Staphylococcus aureus* (*S. aureus*)-ATCC 6538, and gram negative bacterium, *Escherichia coli* (*E. coli*)-ATCC 8739, were used as test organisms. Bacterial inoculums were prepared to obtain bacterial suspension in exponential growth of 10^8 colony forming units (CFU) ml^{-1} in 5 ml nutrient broth (modified Tryptonsoya broth from Oxoids). Atryptone soya agar (from Oxoids) was used as nutrient agar for agar plates. Antibacterial test was carried out on several batches of ORC gauzes coated with N, O-CS. The untreated cotton gauze was used as control

sample. The circular fabric swatches were cut to 4 cm in diameter and then sterilized under Co^{60} irradiation. Each fabric sample was placed in a flask. Antibacterial test was performed according to the AATCC 100-2004 test standard. A series of diluted solutions were prepared as 10^0 , 10^1 , 10^2 , and 10^3 times with sterile distilled water. Then they were plated (3 of each) and incubated for 18 h-24 h at 37 °C. After incubation, the sample with 10^2 dilution was chosen to compare the treated and untreated samples. The plates corresponding to 10^0 and 10^1 times colonies were uncountable and that for 10^3 times had too few colonies for the untreated control sample. The reduction percentage of bacteria by the gauze specimen treatment was calculated through the following formula²⁴⁻²⁶:

$$\text{Reduction in CFU (\%)} = (C_t - T_t) / C_t \times 100 \% \quad (8)$$

Where, C_t : Average number of bacterial colony in untreated cotton gauze; T_t : Average number of bacterial colony in ORC gauze treated with N, O-CS.

Hemostatic evaluation

The hemostatic behavior of the N, O-CS/ORC composite gauzes was estimated by covering gauze on the abraded liver of the male New Zealand White rabbits (which is 4 months old and around 3.5 kg). The neat ORC and N, O-CS/ORC gauzes were cut into pieces of required size (2.0 cm×2.0 cm) and sterilized by ultraviolet radiation for testing the hemostatic efficiency. Before undergoing an abdominal incision, the rabbits were fixed on the surgical cork board and anaesthetized with an intraperitoneal injection of 3 % pentobarbital sodium aqueous solution (30 mg/kg). The neat ORC and its composite gauzes were applied to the liver wound immediately when the liver was pricked with a needle (the diameter is 2 mm, and the pricked depth is 3 mm), respectively. In this step, after three minutes for blood penetration in the samples and easily observed the clot formation on the surface of specimens.

Results

Synthesis of N, O-carboxymethyl chitosan (N, O-CS)

N, O-CS, a derivative of chitosan, was synthesized by the introduction of carboxymethyl groups into N-terminal and O-terminal of CS as showed in Fig. 1. The determined substitution (DS) degree of N, O-CS was up to 1.68. The free

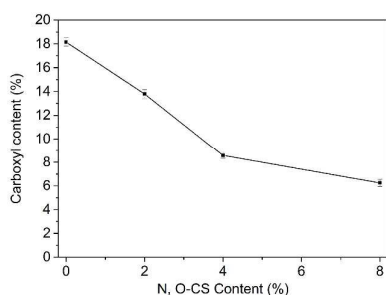


Fig. 4 The relationship between carboxyl content and different N, O-CS content.

Table 1 The data of elemental analysis

Sample	C %	H %	N %
ORC	39.72 ± 0.15	5.13 ± 0.13	-
2 % N, O-CS	34.63 ± 0.28	4.91 ± 0.34	1.20 ± 0.15
4 % N, O-CS	34.52 ± 0.18	5.21 ± 0.20	1.40 ± 0.30
8 % N, O-CS	34.85 ± 0.33	5.24 ± 0.19	1.52 ± 0.28

amine group content after the carboxymethylation of chitosan was 17.03 %. Carboxymethyl group was mainly introduced into OH at C6 and C3 with a small number of NH_2 at C2 ($\text{DS}_O/\text{DS} > 50\%$). The goal of preparing N, O-CS with high DS_O and low DS_N was realized and the antibacterial activity of chitosan was not influenced seriously.²⁷ Due to the fact that nucleophilic substitution reaction of NH_2 at C2 could not only react with OH at C6 but also react with OH at C3. The electronegativity of O was stronger than N. And the steric hindrance of OH at C6 is the smallest. Therefore, the sequence of substitution site was: $\text{OH-6} > \text{OH-3} > \text{NH}_2\text{-2}$.²⁸

Carboxyl content of composite gauzes

Oxidized regenerated cellulose was obtained by NO_2/CCl_4 selective oxidation of viscose gauze, leading to the formation of ORC which contain the carboxyl group. Fig. 4 showed that carboxyl content decreased from 18.15 % to 6.25 % while the content of N, O-CS increased from 0 to 8 %. This phenomenon might be caused by a chemical reaction between N, O-CS and ORC gauze, emerging new chemical bonds.

Elemental analysis

Elemental analysis can be employed to analyse the compositions of the N, O-CS/ORC gauzes and ORC. The results were listed in Table 1, showing that nitrogen proportion increased ranging from 1.20 to 1.52 % with the increase of the N, O-CS content (2 % to 8 %). The results proved in the formation of new chemical bonds (amide bond) between N, O-CS and ORC gauze.

FT-IR

As shown in Fig. 5 a, chitosan showed its unique characteristic peaks at 3435, 1658, 1075 and 1030 cm^{-1} , which were attributed to the stretch and vibration of O-H, N-H, amino group (NH_2 deformation), the second hydroxyl group (C-O) and primary hydroxyl group (C-O-C), respectively.²⁹ In contrast, the spectrum of N, O-CS showed characteristic peaks at 1606 and 1412 cm^{-1} corresponding to carboxylic acid salt ($-\text{COO}^-$ asymmetric stretch) and $-\text{COONa}$ stretch, which showed the exist of carboxymethyl groups on N, O-CS. Furthermore, peaks at 1075 and 1030 cm^{-1} represented secondary hydroxyl group ($-\text{CH-OH}$, C-O) and the primary hydroxyl group ($-\text{CH}_2\text{-OH}$, C-O), respectively because the secondary hydroxyl group was not affected by the modification of chitosan. The results showed that the peak intensity ratio ($1030\text{cm}^{-1}/1070\text{cm}^{-1}$) of N, O-CS

decreased compared with that of CS.²² Demonstrating the substitute of carboxymethyl group for $-\text{CH}_2\text{-OH}$ at C6 position

of N, O-CS. Compared with the $^1\text{H-NMR}$ spectrum of N, O-CS

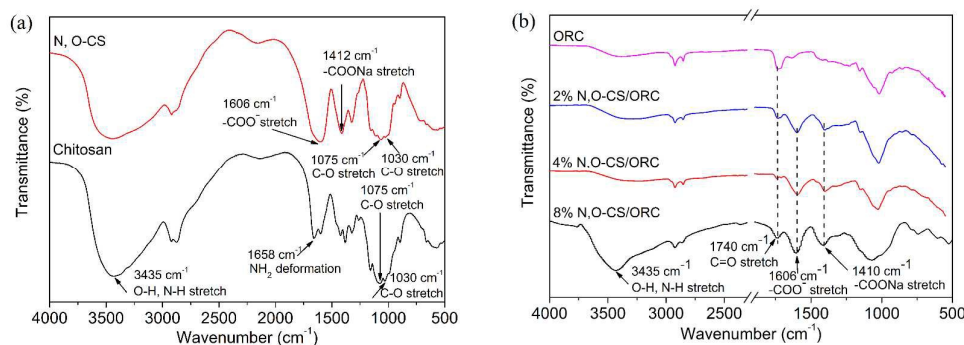


Fig. 5 (a) FT-IR spectra of chitosan and N, O-CS, (b) FT-IR spectra of ORC and composite gauzes with different N, O-CS content.

(Fig.S1, ESI), we observed new signals at 2.6 ppm in the spectrum of N, O-CS. This corresponds to the carboxymethyl group grafted onto the NH_2 at C2 and OH at C6, which was consistent with a previous research.²³

Characteristic absorption band of the ORC clearly appeared at 1740 cm^{-1} due to stretching vibration of C=O ($-\text{COOH}$ group). Treated with N, O-CS, peaks at 1606 and 1410 cm^{-1} corresponding to carboxylic acid salt ($-\text{COO}^-$ asymmetric stretch and $-\text{COONa}$ symmetry stretch), showed that the existence of carboxymethyl group (Fig. 5 b). The spectrums of composite gauzes with different N, O-CS content were similar. And the absorption strength became strong with the increase of N, O-CS content. The absorption strength at 1740 cm^{-1} was weak, but still could be seen with the increase of N, O-CS content (showed in Fig. 5 b), implying that amide bond (O=C-N bond) formed between $-\text{COOH}$ groups in ORC and amino groups in N, O-CS. Compared with the spectrum of pure ORC, O-H and N-H stretching peaks at 3415 cm^{-1} in N, O-CS/ORC gauze became wider and shifted to higher wave number, which showed the existence of the interaction between N, O-CS and ORC gauze.

XRD

X-ray diffraction of N, O-CS, chitosan, composite gauzes was seen in Fig. 6. It showed that the XRD profiles of chitosan exhibited typical diffraction angle (2θ) around at 20.1° , while

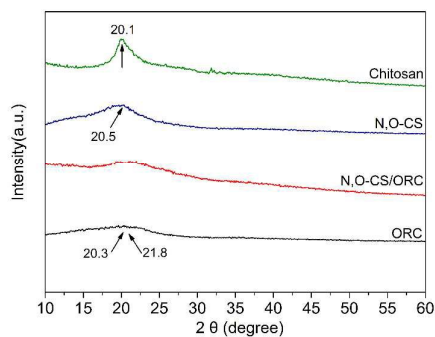


Fig. 6 XRD of chitosan, N, O-CS, ORC, and N, O-CS/ORC composite gauze.

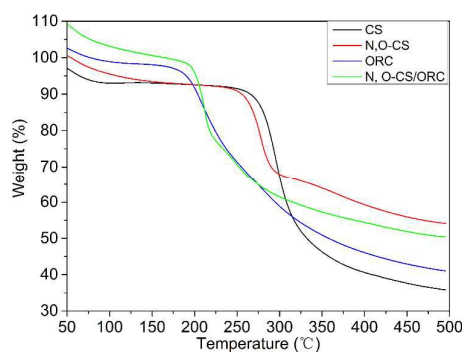


Fig. 7 TGA curves of chitosan, N, O-CS, ORC, and N, O-CS/ORC composite gauze.

N, O-CS typical diffraction angle (2θ) around at 20.5° and almost amorphous. Because of the introduction of carboxymethyl group, distance between molecular chains and destroyed the original crystal structure sharply increased.³⁰ XRD diffraction peaks of ORC showed two weak typical diffraction angles (2θ) around at 20.3° and 21.8° , respectively. The reason is that the crystallinity structure of ORC destroyed during the oxidation reaction and almost be amorphous structure. The peaks became lower diffraction angle apparently in composite gauze and the intensity of diffraction peaks weakened after the N, O-CS coated, which demonstrated that there occurred interaction between the N, O-CS and ORC gauze.

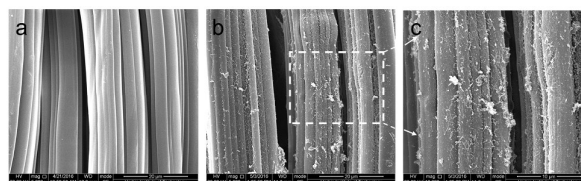


Fig. 8 SEM images of ORC and N, O-CS/ORC fibers. (a) ORC fibers. (b) N, O-CS/ORC fibers (5000 \times). (c) N, O-CS/ORC fibers (10000 \times).

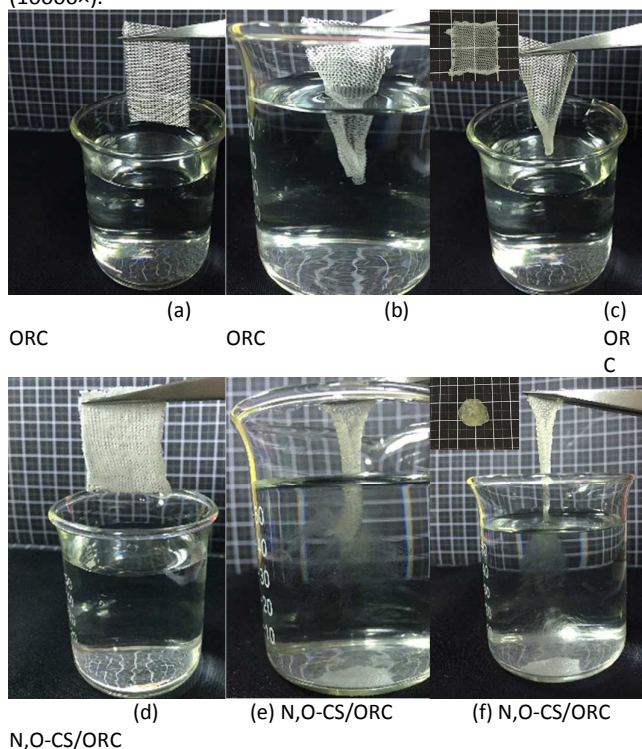


Fig. 9 The digital pictures of N, O-CS/ORC gauze before and after coated N, O-CS dissolved in water. (a), (b), (c) before coated. (d), (e), (f) after coated.

TGA

TGA of chitosan, N, O-CS, ORC and N, O-CS/ORC composite gauze were carried out to evaluate their degradation profiles and thermal stability. TGA curves were shown in Fig. 7. The thermo gravimetric of chitosan, TGA curve of pyrolysis process could be divided into two weight loss stages, consistent with the slow pyrolysis processes (50-100 $^{\circ}\text{C}$) and first pyrolysis (250-400 $^{\circ}\text{C}$) stages, respectively. At the first stage, the mass loss was contributed to volatilization of water. The maximum rate of weight loss was observed in the second stage, where over 56 % weight was pyrolyzed between 250 $^{\circ}\text{C}$ and 400 $^{\circ}\text{C}$. In contrast, TGA curve of N, O-CS could also be divided into two stages, the thermal stability of N, O-CS was weaker than that of chitosan since the onset of thermal degradation of N, O-CS was about 225 $^{\circ}\text{C}$. And the maximum rate of weight loss of N, O-CS was only about 23.9 % between 225 $^{\circ}\text{C}$ and 300 $^{\circ}\text{C}$.²⁴ Due to the process of carboxymethylation together with the rupture of macromolecule chains of chitosan by alkali and high temperature. Moreover, the above factors contributed to the decrease and even damage of polymerization degree of chitosan. Therefore, chitosan had not only better thermo stability than N, O-CS, but also higher pyrolysis than N, O-CS.

The concentration of N, O-CS on surface of ORC was estimated using TGA. As shown in Fig. 7, the maximum thermal degradation temperature of ORC before and after coated N, O-CS was about 200 $^{\circ}\text{C}$. And the maximum rate of weight loss of before and after N, O-CS coated ORC decreased (56.97 % and 48.74 %) between 200 and 300 $^{\circ}\text{C}$, which further demonstrated the formation of chemical bond between N, O-CS and ORC consistent with FT-IR and XRD data.

SEM

Composite gauzes with various N, O-CS content were examined by SEM as presented in Fig. 8. Surface morphology of ORC fibers was rough (Fig. 8 a). Meanwhile, coated happened on composite gauzes, and a layer of N, O-CS was absorbed on the surface of ORC fibers, implying that N, O-CS was connected with ORC fibers during the modification. Also, it can be seen that some of the N, O-CS grains were connected two neighbour ORC fibers to each other. This effect promises increasing the antibacterial and hemostatic properties of ORC fibers (Fig. 8 b & c).

Characterization of water-soluble N, O-CS-coated ORC gauze

In second stage, after N, O-CS coated ORC gauze, N, O-CS/ORC

Table 2 The bactericidal properties of different N, O-CS/ORC gauze

Samples	<i>S. aureus</i> (%)	<i>E. coli</i> (%)
ORC	> 94.65	> 92.89
2%N, O-CS/ORC	> 95.66	> 93.57
4%N, O-CS/ORC	> 97.38	> 95.25
8%N, O-CS/ORC	> 99.99	> 97.68
Surgical	> 99.99	> 99.99

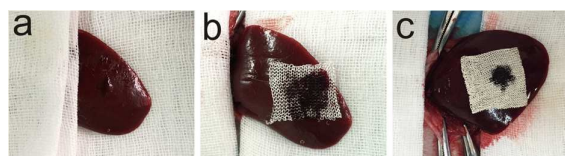


Fig. 10 Images of injured site of rabbit liver (a), hemostatic evaluation of neat ORC (b) and N, O-CS/ORC composite gauze (c).

gauze was neutralized to gain the water-soluble sodium salts. Water soluble characteristics of N, O-CS-coated ORC composite gauze were given in Fig. 9.³¹ Saferstein et al. discovered that neutralizing oxidized cellulose cloth in aqueous solutions of sodium bicarbonate led to that was partially gelled, distorted from its original size, very weak, with little integrity. The tensile strength of the cloth was too low to use as a hemostat in surgery. While in our experiment, comparing

Fig. 9 a & d, we could find that after N, O-CS coated ORC gauze, the composite gauze totally lose their original physical forms and generate transparent gel quickly for 10 s after the gauzes are soaked with enough water (Fig. 9 e & f). This is due to the N, O-CS coated ORC gauze, the sodium carboxylate (COONa) groups have been introduced into the materials, which are water-soluble. Thus, N, O-CS/ORC composite gauze could be dissolved in an aqueous solution, while the gauze before the N, O-CS coated could not be dissolved into the aqueous solution and only swelling behavior in aqueous solution (Fig. 9 b & c).

Antibacterial Activity Test

Antibacterial activity of ORC and N, O-CS/ORC gauzes was evaluated against Gram positive and negative bacteria, *S. aureus* and *E. coli*. The results were indicated in Table 2. The inhibitory rate against *S. aureus* and *E. coli* was apparently increased with the increase of N, O-CS content. It implied that the strong antibacterial activity of N, O-CS compensated for the decreasing antibacterial property of ORC during consumed some -COOH groups. Most researchers reported that the antibacterial property of ORC depended on its pH. Lower pH gave better antibacterial property of ORC. In addition, most literatures^{25, 26} reported that chitosan killed bacteria through damage to the cell membrane and these damages were caused by electrostatic interactions between chitosan protonated amino groups and phosphoryl groups of phospholipid components of cell membranes. And the inhibitory rate against *S. aureus* was higher than *E. coli* with identical same N, O-CS content.

Hemostatic Capability

There were several factors affected the bleeding of the white rabbit liver. For example, the blood pressure and wound size of the liver. In order to reduce experimental error, three rabbits for each specimen were used. Results of hemostatic capability were shown in Fig. 10. The rabbit livers experiments indicated that both of neat ORC and N, O-CS/ORC composite gauze could stop bleeding and decreased blood coagulation on the surface of liver. Used of N, O-CS/ORC composite gauze stopped bleeding in 90 seconds, while there was still bleeding points in ORC gauze (stopped bleeding in 4 minutes). The average blood uptake of neat ORC was 359.8 % and that of N, O-CS/ORC was 128.1 %. The reasons for this phenomenon: Firstly, the unreacted -COOH groups in ORC had the capability to bind with Fe³⁺ in blood fluid to form the brown gel. Secondly, the water-soluble -COONa groups would absorb water from the blood and make the gauze quickly gel. And concentrate the clotting factors to carry out hemostatic. In this way, rapid coagulation rate would make a smaller amount of blood loss and clots formation. As we all know, the clot will affect the efficacy of tissue anti-adhesion. It indicated that N, O-CS/ORC composite gauzes, which are beneficial for postoperative adhesion prevention.

Conclusions

In this research, a novel technique was invented to graft ORC with a water-soluble N, O-CS via amide bonds. At first, N, O-CS was successfully prepared by modifying chitosan with chloroacetic acid in alkaline solution. Then, ORC gauze was coated with the above N, O-CS. The formation of amide bond between the carboxyl group of ORC and the amino group of N, O-CS was confirmed by FT-IR and Elemental analysis. Antibacterial properties of N, O-CS/ORC composite gauzes increased with the increasing of N, O-CS content. The N, O-CS coated ORC gauze was water-soluble and was able to form gel by absorbing blood and then seals off the crevasses of blood vessels to stop bleeding. This research indicated that the hemostatic performance of ORC can be improved by introducing a small proportion of N, O-CS. The notable properties of N, O-CS/ORC composite gauzes have promising future applications in reducing the formation of postoperative adhesions after surgery.

Acknowledgments

This work was financially supported by State Key Laboratory for Modification of Chemical Fibers and Polymer Materials, Donghua University (No. LK1510).

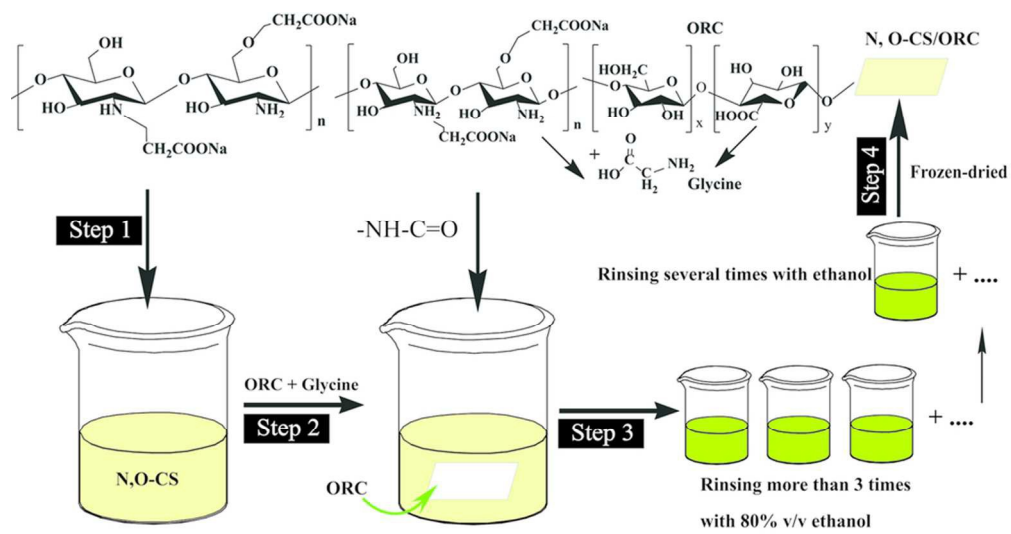
Notes and references

- 1 M. N. V. R. Kumar, *React Funct Polym*, 2000, **46**, 1-27.
- 2 L. H. Zhu, V. Kumar, G. S. Banker, *Int J Pharm*, 2001, **223**, 35-47.
- 3 H. Wang, M. Li, J. Hu, C. Wang, S. Xu and C. C. Han, *Biomacromolecules*, 2013, **14**, 954-961.
- 4 Q. Xia, Z. Liu, C. Wang, Z. Zhang, S. Xu and C. C. Han, *Biomacromolecules*, 2015, **16**, 3083-3092.
- 5 Y. C. Chung, Y. P. Su, C. C. Chen, G. Jia, H. I. Wang, J. C. G. Wu and J. G. Lin, *Acta Pharmacol Sin*, 2004, **25**, 932-936.
- 6 E. Lih, S. H. Oh, Y. K. Joung, J. H. Lee and D. K. Han, *Prog Polym Sci*, 2015, **44**, 28-61.
- 7 B. C. Ward, S. Kavalukas, J. Brugnano, A. Barbul and A. Panitch, *J Surg Res*, 2011, **169**, e27-36.
- 8 G. M. Boland and R. J. Weigel, *J Surg Res*, 2006, **132**, 3-12.
- 9 A. M. Abdelgawad, S. M. Hudson and O. J. Rojas, *Carbohydr Polym*, 2014, **100**, 166-178.
- 10 R. A. A. Muzzarelli, P. Morganti, G. Morganti, P. Palombo, M. Palombo, G. Biagini, M. Mattioli Belmonte, F. Giantomassi, F. Orlandi and C. Muzzarelli, *Carbohydr Polym*, 2007, **70**, 274-284.
- 11 K. Sun, *Express Polym Lett*, 2011, **5**, 342-361.
- 12 G. Toskas, C. Cherif, R. D. Hund, E. Laourine, B. Mahltig, A. Fahmi, C. Heinemann and T. Hanke, *Carbohydr Polym*, 2013, **94**, 713-722.
- 13 F. Cheng, J. Gao, L. Wang, X. Y. Hu, *J Appl Polym Sci*, 2015, **132**, 42060.
- 14 M. G. McKee, J. M. Layman, M. P. Cashion and T. E. Long, *Science*, 2006, **311**, 353-355.
- 15 A. J. Varma, S. V. Deshpande and J. F. Kennedy, *Carbohydr Polym*, 2004, **55**, 77-93.
- 16 T. J. Krause, G. A. Zazanis and R. D. McKinnon, *Wound Repair Regen*, 1996, **4**, 53-57.
- 17 J. Zhou, J. M. Lee, P. Jiang, S. Henderson and T. D. G. Lee, *J Thorac Cardiovasc Sur*, 2010, **140**, 801-806.
- 18 J. Zhou, R. S. Liwski, C. Elson and T. D. G. Lee, *J Thorac Cardiovasc Sur*, 2008, **135**, 777-783.

ARTICLE

RSC Advances

- 19 J. M. He, F. W. Wang, Y. D. Wu, Y. D. Huang and H. W. Zhang, *Cellulose*, 2011, **18**, 1651-1659.
- 20 A. N. Chakoli, J. M. He, W. L. Cheng and Y. D. Huang, *RSC Adv.*, 2014, **4**, 52372-52378.
- 21 W. L. Cheng, J. M. He, Y. D. Wu, C. Song, S. S. Xie, Y. D. Huang and B. Fu, *Cellulose*, 2013, **20**, 2547-2558.
- 22 S. C. Chen, Y. C. Wu, F. L. Mi, Y. H. Lin, L. C. Yu and H. W. Sung, *J Control Release*, 2004, **96**, 285-300.
- 23 L. Li, N. Wang, X. Jin, R. Deng, S. H. Nie, L. Sun, Q. J. Wu, Y. Q. Wei and C. Y. Gong, *Biomaterials*, 2014, **35**, 3903-3917.
- 24 X. Zheng, H. Zhang, Y. She and J. W. Pu, *J Appl Polym Sci*, 2014, **131**, 39851.
- 25 Y. D. Wu, J. M. He, F. W. Wang, W. L. Cheng, Y. D. Huang and B. Fu, *Fiber Polym*, 2014, **15**, 504-509.
- 26 J. M. He, Y. D. Wu, Y. D. Huang, F. W. Wang and F. Tang, *Fiber Polym*, 2012, **13**, 576-581.
- 27 I. Aranaz, M. Mengibar, R. Harris, I. Paños, B. Miralles, N. Acosta, G. Galed, Á. Heras, *Curr Chem Biol*, 2009, **3**, 203-230.
- 28 H. K. Chun, J. W. Choi, J. C. Heung and S. C. Kyu, *Polym Bull*, 1997, **38**, 387-393.
- 29 K. Mladenovska, R. S. Raicki, E. I. Janevik, T. Ristoski, M. J. Pavlova, Z. Kavrakovski, M. G. Dodov and K. Goracinova, *Int J Pharm*, 2007, **342**, 124-136.
- 30 C. Zhang, Q. E. Ping, H. J. Zhang and J. Shen, *Eur Polym J*, 2003, **39**, 1629-1634.
- 31 L. Saferstein, S. Wolf, L. Kamp, C. Linsky and D. Wiseman, *US patent*, 1992, 5134229.



43x22mm (600 x 600 DPI)